High-sensitivity X-ray polarimetry with amorphous silicon active-matrix pixel proportional counters

J.K. Black*[a], P. Deines-Jones[b], K. Jahoda[c], S.E. Ready[d], R.A. Street[d]

[a] Forbin Scientific, Code 662, NASA/Goddard Space Flight Center, Greenbelt, MD, 20771, USA
[b] Universities Space Research Association, Code 662, NASA/Goddard Space Flight Center
[c]Laboratory for High-Energy Astrophysics, Code 662, NASA/Goddard Space Flight Center
[d] Palo Alto Research Center, 3333 Coyote Hill Road, Palo Alto, CA, 94304 USA

ABSTRACT

Photoelectric X-ray polarimeters based on pixel micropattern gas detectors (MPGDs) offer order-of-magnitude improvement in sensitivity over more traditional techniques based on X-ray scattering. This new technique places some of the most interesting astronomical observations within reach of even a small, dedicated mission. The most sensitive instrument would be a photoelectric polarimeter at the focus of a very large mirror, such as the planned XEUS. Our efforts are focused on a smaller pathfinder mission, which would achieve its greatest sensitivity with large-area, low-background, collimated polarimeters. We have recently demonstrated a MPGD polarimeter using amorphous silicon thin-film transistor (TFT) readout suitable for the focal plane of an X-ray telescope. All the technologies used in the demonstration polarimeter are scalable to the areas required for a high-sensitivity collimated polarimeter.

Keywords: X-ray polarimetry, particle tracking, proportional counter, GEM, pixel readout

1. INTRODUCTION

The recent introduction of a high-sensitivity photoelectric X-ray polarimeter[1-3] has created new possibilities for extracting important and unique information about astrophysical systems. However, some of the most interesting objects, such as active galactic nuclei, have source fluxes equivalent to only a few milliCrab, and are expected to have fractional polarizations of a few-percent. In this paper, we describe how to reach the goal of measuring such sources in a small pathfinder mission using large-area collimated detectors.

This new type of polarimeter uses a finely spaced, gas pixel detector to image the tracks of photoelectrons. Polarization information is obtained by determining the angle of emission of the photoelectron, which is correlated with the electric field vector of the X-ray. The primary technical innovation is the introduction of a pixel readout anode to a micro-pattern gas detector (MPGD). With a pixel size small compared to the photoelectron range, photoelectron tracks are imaged and the emission angle reconstructed event-by-event. Combined with the high quantum efficiency and broad bandpass of the photoelectric effect, this technique gives dramatic improvements in sensitivity over polarimeters based on X-ray scattering[4].

A small mission could achieve greatest polarization sensitivity to sources at or above one milliCrab with ~5000 cm^2 of collimated polarimeters. Measuring few-percent polarization of sources fainter than about one milliCrab will require a polarimeter at the focus of a very large X-ray telescope such as the planned XEUS[5]. However, polarimetry above the milli-Crab level does not require the high-resolution imaging or background reduction afforded by a focusing optic, yet X-ray optics come at a large cost in efficiency. Even at their most efficient, the effective area of X-ray mirrors is less than 25 per cent of their geometric area. In a small mission with a fairly short focal length (2 meter), the effective area is further degraded above a few keV.

Such a large-area photoelectric polarimeter requires both pixel proportional counters and active pixel readout. Both are commercially available technologies. Large-area micropattern proportional counters have been developed primarily for applications in high-energy physics and have recently been introduced as a commercial product[6]. Active-matrix pixel readouts using amorphous silicon thin-film transistor (TFT) arrays have been used in flat-panel medical imagers[7] for several years.

As a first step toward a large-area instrument, we have demonstrated a MPGD polarimeter with TFT active-matrix readout. We describe these results and discuss the sensitivity possible in a pathfinder mission with a large-area polarimeter.

2. TECHNOLOGY DEMONSTRATION

Using a MPGD with a TFT readout, we recently recorded photoelectron track images from 5.9 and 20 keV X-rays and made polarization measurements at 4.5 keV[8]. The detector, shown schematically in Figure 1, consisted of a double-GEM[9] with 100-μm hexagonal pitch and a TFT pixel anode with 100-μm square pitch. The active area was defined by the double-GEM, which was 12mm x 12mm. Only a small fraction of the TFT array's 512 x 512 pixels (about 25 cm^2) was used. We did not align the GEMs with each other or with the TFT array.

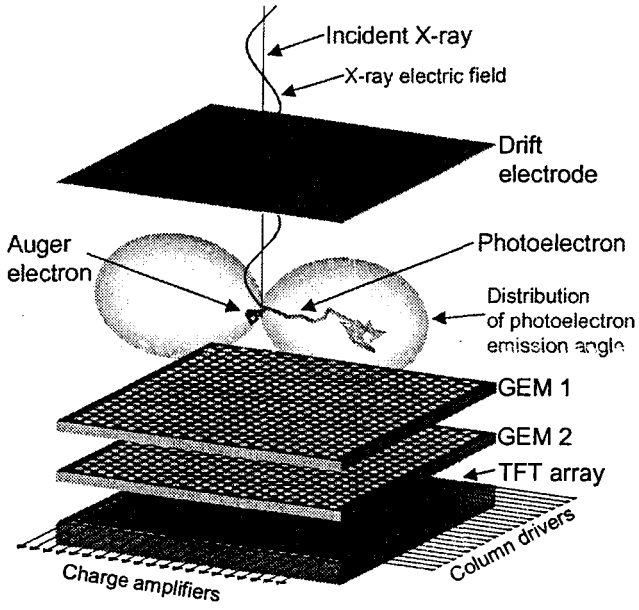

Figure 1. Schematic diagram of detector geometry used in these measurements. The $\sin^2\theta\cos^2\phi$ distribution of photoelectron emission for normally incident X-rays is projected onto the detector plane and observed as $\cos^2\phi$.

The GEMs were contained in a detector body with a thin polyimide entrance window. The active depth was 3mm, determined by the spacing between a nickel mesh drift electrode and the GEMs. The spacing between GEMs was 750 μm. The spacing between the GEMs and the TFT array was maintained by a 750 μm thick silicone gasket that also acted as a gas seal. The detector was operated as a flow counter using an 80% neon, 20% CO_2 gas mixture at an apparent gain of about 10^4. The drift field was 300 V/cm.

We fabricated the GEMs by UV laser ablation[10,11] in the Laboratory for High Energy Astrophysics at NASA's Goddard Space Flight Center (GSFC). The GEMs are 75 μm thick with hole diameters that are 60 μm at the electrodes, constricting to 50 μm in the center of the substrate.

The TFT pixel arrays were fabricated at the Palo Alto Research Center using a process scalable to large areas (~10

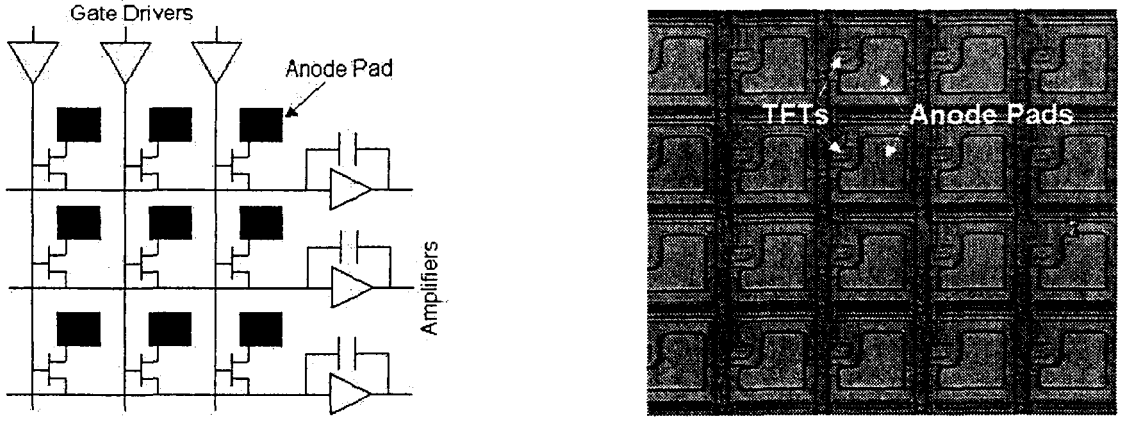

Figure 2. (Left) The TFT active-matrix readout scheme is highly scalable. (Right) Optical microscope photo of the array used in these measurements. The pixels are on a 100 micron spacing.

cm^2). Each pixel contains a metal anode pad, a storage capacitor of about 0.4 pF and a TFT switch[12,13]. The source of the TFT is connected to the anode pad, which is isolated from the rest of the pixel by an insulation layer. The TFT gates are connected in columns and the drains are connected in rows as shown in Figure 2. With the TFT switches open, charge from the GEMs is stored on the anode pads. To read out the array, the TFT switches are closed column-by-column by activating the gates lines, so that charge is transferred from a column of anode pads to a row of external amplifiers[7].

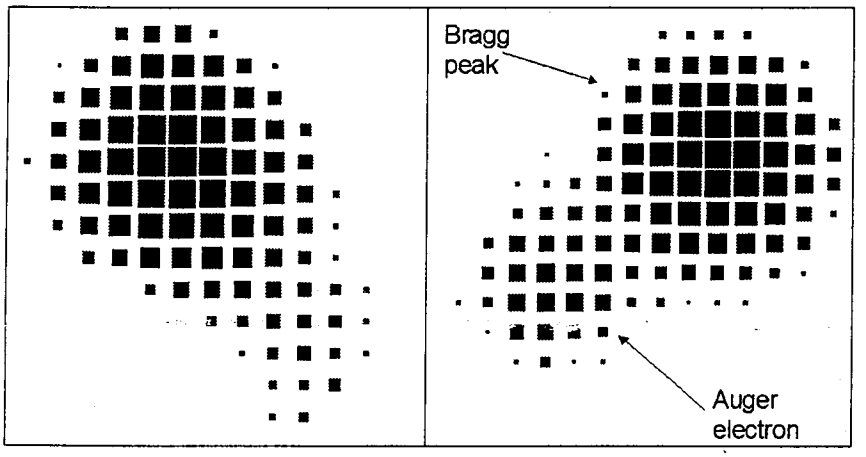

Figure 3. Example track images from 5.9 keV X-rays. The boxes are on a 100 micron grid. The area of each box represents the total charge collected in the pixel. Two peaks are visible in the distribution. The smaller peak is due to the Auger electron, emitted at the X-ray interaction point.

Figure 3 shows a sample of tracks recorded from 5.9 keV X-rays. Most of the charge is deposited at the end of the photoelectron track. At the beginning of the track is a smaller cluster of charge deposited by the Auger electron (870 eV in neon), which is emitted isotropically. Significantly more structure is seen in tracks from 20 keV photons as shown in Fig. 4. The Auger/interaction point can still be identified among more hard scatters and knock-on electrons. At 4.5 keV most of this fine structure is obscured by the diffusion of the primary electrons in the drift volume as shown in Figure 4. Nevertheless, the track images have a discernable direction.

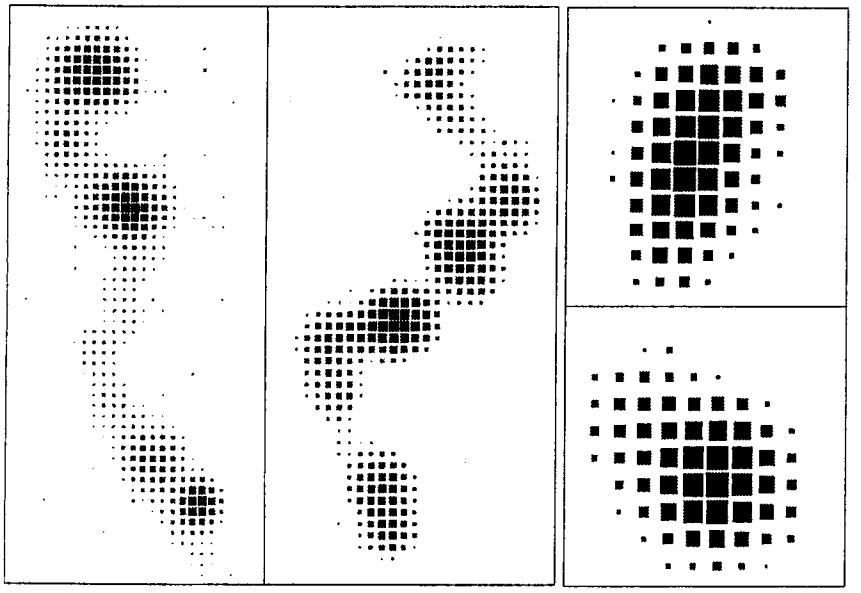

Figure 4. Track images from 20 keV X-rays (left) and 4.5 keV X-rays (right).

We produced polarized photons by reflecting X-rays at 90 degrees off a silicon crystal. The X-rays were produced by a tube with a titanium anode (K_α = 4.5 keV). The X-ray tube and crystal were mounted on a swivel arm that allowed the plane of polarization to be rotated with respect to the detector coordinate system as shown in Figure 5. Data were collected with the plane of X-ray polarization (ϕ_{pol}) at three different angles, separated by about 45 degrees.

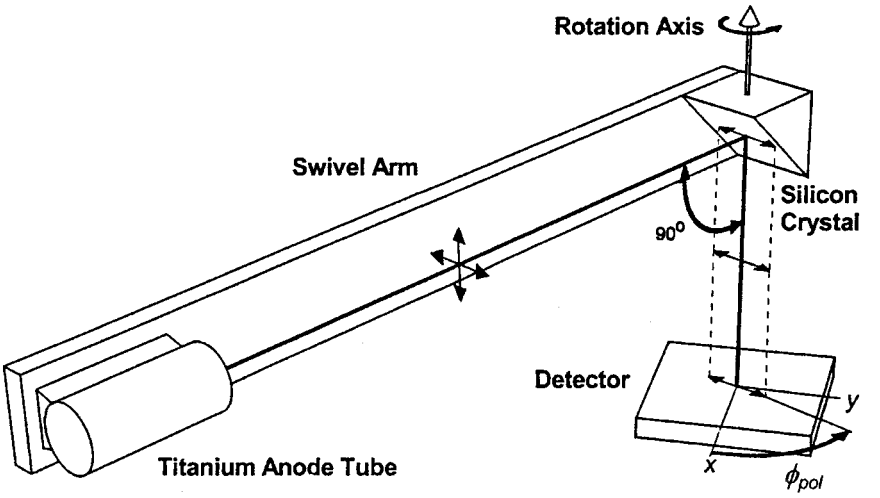

Figure 5. Experimental setup for polarization measurements. Polarized X-rays at 4.5 keV were produced by scattering at 90^0 off a silicon crystal mounted above the detector. The tube and crystal were mounted on a swiveled arm that allowed the plane of polarization to be rotated with respect to the detector coordinate system by the angle ϕ_{pol}.

We analyzed the polarized data first by reconstructing the emission angle of each photoelectron. We then fit histograms of the emission angles to the expected functional form: $N(\phi) = A + B\cos^2(\phi - \phi_{pol})$, where ϕ_{pol} is the angle of the plane of polarization. The ability of an analyzer to distinguish polarized from unpolarized light is defined as its modulation factor μ, the observed fraction of polarization from a 100% polarized source:

$$\mu = (N_{max} - N_{min})/(N_{max} + N_{min}) = B/(2A + B),$$

where N_{max} and N_{min} are the maximum and minimum of the function, respectively.

We estimated the direction of photoelectron emission of each event as the direction of the major axis of the second moment of the charge distribution. Specifically, we calculated the angle of emission as the angle ϕ that minimized the second moment M of the total charge distribution with barycenter coordinates (x_b, y_b):

$$M = \frac{\sum_i q_i[(y_i - y_b)\cos\phi - (x_i - x_b)\sin\phi]^2}{\sum_i q_i}$$

where q_i is the charge in the pixel with coordinates (x_i, y_i). All pixels above a threshold of 2000 electrons (twice the rms noise in the electronics) in a 3.1 x 3.1 mm^2 box centered on (x_b, y_b) were included in the calculation. We did not perform a more refined analysis[14] that attempts to include only the pixels near the interaction point.

The results shown, in Fig. 6, demonstrate the polarization sensitivity of the detector. The data fit the expected functional form and peak around the independently measured polarization angle of the incident X-rays. All three data sets are consistent with the average modulation of 0.33 ± 0.03, which is also consistent with results from simulated data. The fit parameters are given in Table 1.

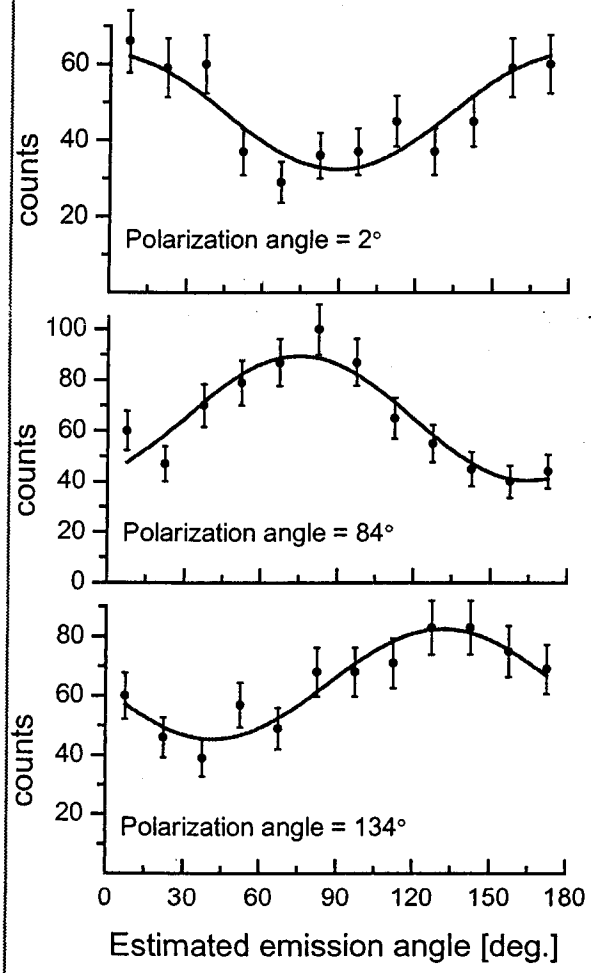

Figure 6. Histograms of reconstructed emission angles for three polarization angles. The curves are fits to the data.

	Fit Parameters	
Polarization Angle	μ	ϕ_{pol}
2	0.30 ± 0.06	0 ± 5
84	0.38 ± 0.05	75 ± 4
134	0.29 ± 0.05	132 ± 5

Table 1. Fit results to reconstructed emission angles. Stated errors are one standard deviation.

3. ESTIMATED SENSITIVITY

The sensitivity of a polarimeter is typically defined in terms of μ by the *minimum detectable polarization* (MDP). MDP is the apparent polarization arising from statistical fluctuations in the measurement of a completely unpolarized source. For an astronomical polarimeter, MDP is a function of the polarimeter properties as well as the source strength S and the observing time t. At the 99% confidence level[15]:

$$MDP = \frac{4.29}{\varepsilon \mu SA}\left(\frac{\varepsilon SA + B}{t}\right)^{\frac{1}{2}}$$

where ε = quantum efficiency, A = collecting area, B = background rate (internal and diffuse) and E = photon energy. In the strong source approximation (S >> B), the MDP scales with instrument parameters as $1/\mu\sqrt{\varepsilon A}$.

3.1 Large-area polarimeter instrument concept

The collimated polarimeter concept is schematically illustrated in Figure 7. The instrument consists of modules of ~500 cm^2 each. The collimators each consist of two orthogonal sets of slats. Inside the detector body are MPGDs with TFT readout arrays, and anti-coincidence MPGD behind the TFT arrays for background rejection.

Large-area MPGDs are a demonstrated technology. Micropattern detectors have been developed mainly in high-energy physics experiments for charged-particle tracking. For example, the COMPASS experiment has twenty 31x31 cm^2 GEMs[16]. The 3M Corporation's Microinterconnect Systems Division can produce 30x30 cm^2 detectors on a commercial basis[6].

Large area TFT arrays are routine in both flat-panel displays and medical imagers. TFT readout arrays are commercially available in large area (10^3 cm^2) that, including all electronics, cost about \$200/cm^2 and consume 20mW/cm^2. For example, Varian Medical Systems markets the PaxScan 2520, a 500 cm^2 readout plane with 127 micron pixels. Another example is GE's DXR series flat panel imagers. The DXR-5000 has an active area of 368 cm^2 with 100 micron pixels and the DXR-250 has 1680 cm^2 with 200 micron pixels.

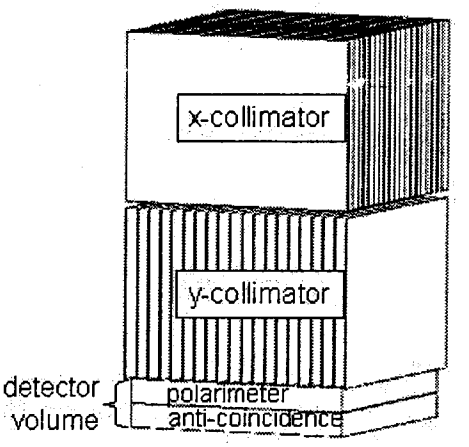

Figure 7. Collimated photoelectric polarimeter module consisting of crossed-slat collimators and pixel proportional counter with anti-coincidence.

A collimator with sufficient angular resolution to limit X-ray background and prevent source confusion. The flux of the diffuse X-ray background is equivalent to about one milliCrab per square degree. A collimator with a 30 arc-min field-of-view would reduce the X-ray background to the expected level of the internal background. A 20 arc-min would virtually eliminate source confusion in all but the most crowded fields and reduce the X-ray background to a small fraction of the internal background. The alignment requirements of a 20 arc min crossed slat collimator are less demanding than of a conical foil mirror.

3.2 Sensitivity estimate

We have estimated the sensitivity in terms of MDP of two polarimeter instrument concepts sized as a dedicated NASA Small Explorer (SMEX) mission. One instrument has our currently demonstrated polarimeters at the focus of conical-foil X-ray telescopes. The other has a large-area collimated polarimeters as described above. The modulation factors used to estimate MDP are based on published simulations[15].

The SMEX X-ray mirror instrument assumes three co-aligned 33 cm diameter mirrors with a 1.8 meter focal length with a total effective area of about 600 cm2 below 2 keV. The polarimeters are optimized to match the mirror response with a 50 micron beryllium window and micropattern polarimeter with 80% DME/20% neon at 380 Torr and a 2 cm depth. The large-area instrument assumes a total active area of 4000 cm^2 with a 75% open fraction (3000 cm^2 effective area) and a 20 arc min (fwhm) collimator. We have again used a 50 micron beryllium window but with the gas mix 80% neon/20% DME at 380 Torr and a 2 cm depth. The 80/20 mix of neon-DME takes greater advantage of the

increased bandpass of the large-area detector. The unrejected internal background is assumed to be the same as the neon-based proportional counters on OSO-8[17].

The estimated sensitivities are shown in Figure 8 are for a 10^5 second observation. Also shown for comparison is the estimated sensitivity of the Stellar X-ray Polarimeter (SXRP), the most sensitive X-ray scattering polarimeter built for astronomical observations. SXRP was to have flown on the Spectrum-X-Gamma mission with the very large effective area (~1400 cm^2) SODART telescope. This illustrates not only the dramatic increase in sensitivity afforded by the new photoelectric polarimeters, but also the potential improvement in sensitivity that could be obtained by the development of large-area photo-electric polarimeters, at least in the constraints of a small mission.

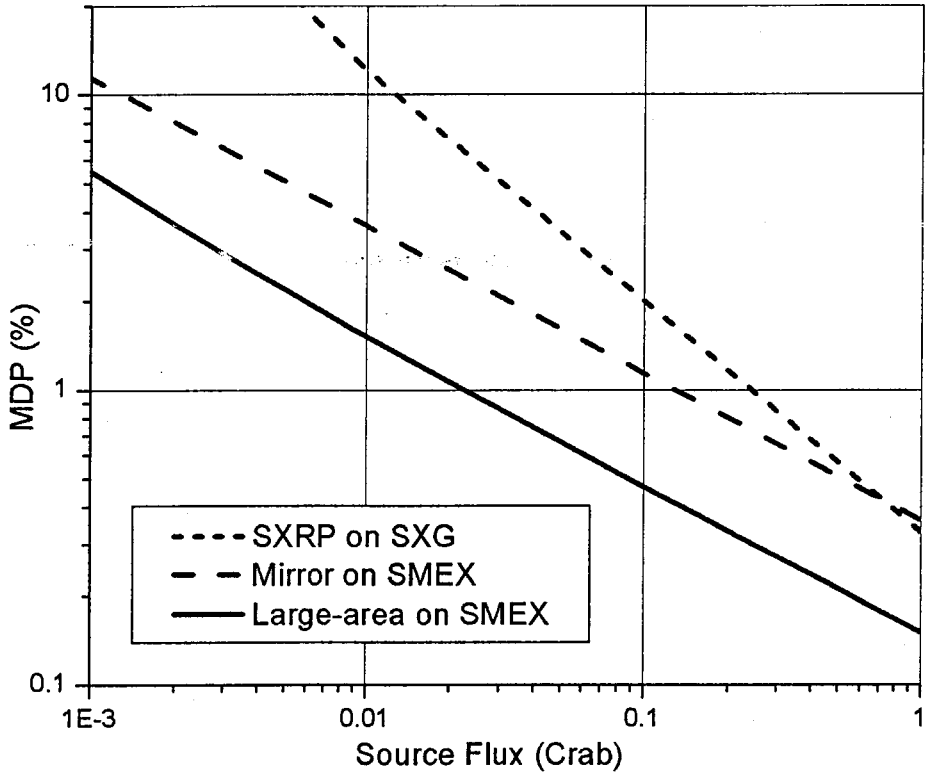

Figure 8. Estimated sensitivites of the two Small Explorer-sized polarimeters considered, one with focusing X-ray optics, the other with large-area collimated detectors. Also shown is the estimated sensitivity of SXRP.

3. CONCLUSION

We have demonstrated a micropattern photoelectric polarimeter with a geometry suitable for the focal plane of an astronomical X-ray telescope. In a small mission, the larger collecting area provided by a collimated instrument compared to an X-ray optic more than compensates for the increased background. The technologies used, particularly amorphous silicon TFT readout, can be scaled to the large areas required for a large-area, low-background, collimated instrument.

4. ACKNOWLEDGEMENTS

This work was funded by NASA grant number NRA-01-01-HEA-021 and the GSFC Director's Discretionary Fund. Numerous individuals in the Laboratory for High Energy Astrophysics at GSFC supported this work. We particularly

thank Mike Lenz, Bert Nahory, Norman Dobson, Drew Jones and Dr. Scott Owens for crucial technical support. We also thank the members of the PARC process line for fabricating the TFT array.

5. REFERENCES

1. E. Costa, P. Soffitta, R. Bellazzini, A. Brez, N. Lumb, G. Spande, "An efficient photoelectric X-ray polarimeter for the study of black holes and neutron stars", *Nature* **411**, pp. 662-665, 2001.
2. R. Bellazzini, G. Spandre, N. Lumb, "Progress with micro-pattern gas detectors," *Nucl. Instr. and Meth.* **478**, pp. 13-25, 2002.
3. R. Bellazzini, et al., "X-ray Polarimetry with a Micro Pattern Gas Detector with Pixel Read Out", *IEEE Trans. Nucl. Sci.* **NS-49**, pp. 1216-1221, 2002.
4. R. Bellazzini, et al., "A Micro Pattern Gas Detector for X-ray Polarimetry", *Proc. SPIE* **4843**, pp. 372-382, 2003.
5. E. Costa, et al., "X-ray Astronomical Polarimetry in the XEUS Era", *XEUS-studying the evolution of the hot universe*, eds. G. Hasinger, Th. Boller, and A.N. Parmer, MPE report 281. p.235, 2002.
6. P.S. Barbeau, J.I. Collar, J.D. Geissinger, J. Miyamoto, "A First Mass Production of Gas Electron Multipliers", submitted to *Nucl. Instr. Meth. A*.
7. R. A. Street, *Technology and Applications of Amorphous Silicon*, Editor R.A. Street, Springer Series in Materials Science 37, Springer-Verlag, Berlin, 2000.
8. J.K. Black, P. Deines-Jones, S.E. Ready, R.A. Street, "X-ray polarimetry with an active-matrix pixel proportional counter", to be published in *Nucl. Instr. Meth. A*.
9. F. Sauli, "GEM: a new concept for electron amplification in gas detectors", *Nucl. Instr. and Meth. A* **386**, pp. 531-534, 1997.
10. J.K. Black, et al., "Imaging microwell detectors for x-ray and gamma-ray applications," *Proc. SPIE* **4140**, pp. 313-323, 2000.
11. P. Deines-Jones, et al., "Large-area imaging micro-well detectors for high-energy astrophysics," *Nucl. Instr. and Meth. A* **478**, pp. 130-134, 2002.
12. R. Street, et al., "X-ray imaging using lead iodide as a semiconductor detector," *Proc. SPIE* **3659**, pp. 36-47, 1999.
13. R. Street, et al., "High-resolution direct-detection x-ray imagers," *Proc. SPIE* **3977**, pp. 418-428, 2000.
14. R. Bellazzini, et al., "Novel gaseous X-ray polarimeter: data analysis and simulation," *Proc. SPIE* **4843**, pp. 383-393, 2003.
15. L. Pacciani, et al., "The sensitivity of a photoelectric X-ray polarimeter for Astronomy: The impact of gas mixture and pressure", *Proc. SPIE* **4843**, pp.394-405, 2003.
16. C. Altunbas et al., "Construction, test and commissioning of the triple-gem tracking detector for compass," *Nucl. Instr. Meth. A* **490**, pp.177-203, 2002.
17. A.N. Bunner , "Soft X-ray Results from the Wisconsin Experiment on OSO-8,", *Ap.J.* **220**, pp.261-271, 1978.